Supplementary Figure 1

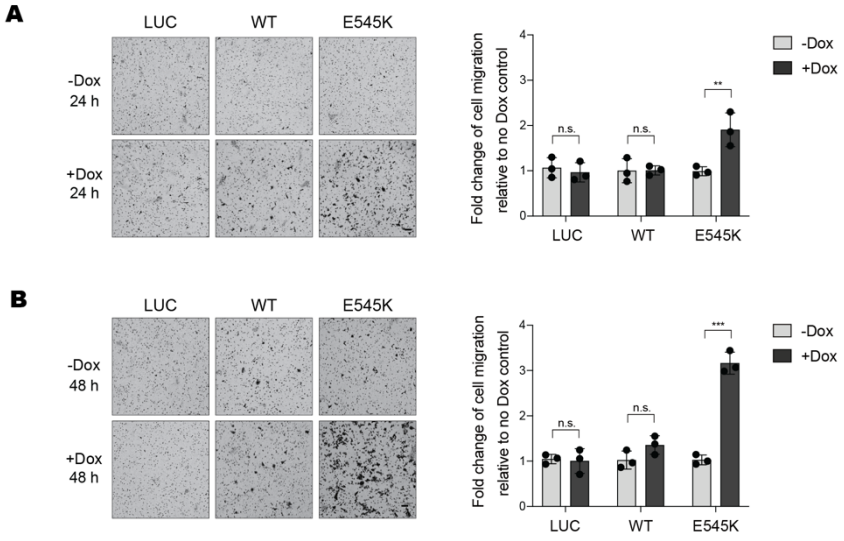

The Q75E *PIK3CA* mutation exhibits an activating phenotype in a HNSCC platform

Cell migration assays. PCI-52-SD1 cells were applied to Boyden chambers and incubated for 24h (**A**) or 48 h (**B**) in the absence or presence of doxycycline (Dox, 1 µg/mL), followed by crystal violet staining. Images were taken from the bottom side of transmembrane chambers. Scale bar, 100 µm. The migrated cells were quantified using ImageJ and the relative cell migration level was normalized to no Dox treatment (n=3). Columns represent the mean ± sd. ***$p < 0.001$, **$p < 0.01$, n.s. ≥ 0.05 for Student's pairwise t-test. The experiments were repeated twice with similar results.

Supplementary Figure 2

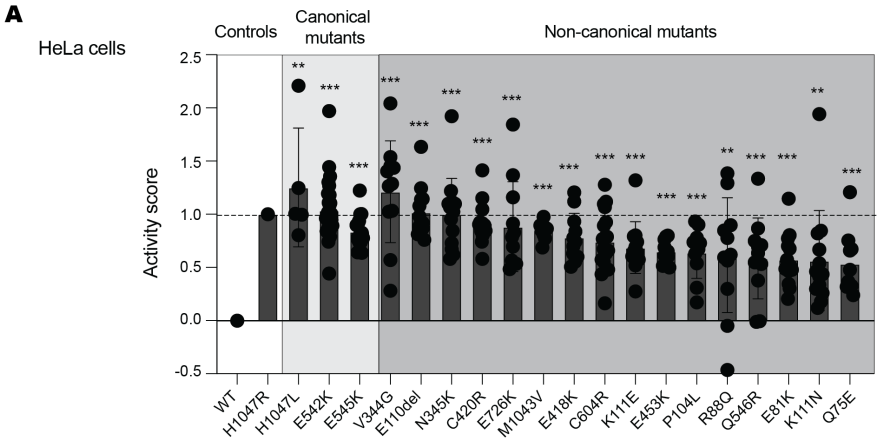

B

	HNSCC model Activating	HNSCC model Non-activating
MCF10A model Activating	22	0
MCF10A model Non-activating	0	10

Kendall's tau coefficient of agreement = 1.00
(95% CI=N/A) (p=<.0001)

	HNSCC model Activating	HNSCC model Non-ctivating
BaF3 model Activating	20	0
BaF3 model Non-activating	2	10

Kendall's tau coefficient of agreement = 0.88
(95% CI= 0.71, 1.00) (p=<.0001)

Functional characterization of all 32 non-canonical *PIK3CA* mutations in HNSCC serum-dependent model

(**A**) Functional assessment of 16 non-canonical *PIK3CA* mutations in HeLa cells using an *in vitro* cell-based assay. HeLa cells were engineered to express a fluorescently tagged FOXO1 transcriptional factor. Cells were then transfected to overexpress WT and mutant *PIK3CA*, followed by fixation and scanning using a fluorescent microscope to detect reporter localization that generated nuclear-to-cytoplasmic ratios (NCR) to provide comparisons between signaling activity for each mutant (n>5). The y-axis of activity score represents NCR values, which were normalized and scored according to the activation levels of *PIK3CA* WT and the canonical *PIK3CA* mutation H1047R (0 represents WT activity and 1 is the activity of the *PIK3CA* H1047R). The dashed line was set as the value equal to the activity of the *PIK3CA* H1047R mutant (1). A mutation was defined as "activating" if the mutation exhibited an activity significantly higher than WT. All mutants were assessed with more than 10 replicates, except for H1047R (n=5). Columns represent

the mean ± sd. ***p < 0.001, **p < 0.01 for Student's pairwise t-test. (**B**) Correlation analysis between the functional data from the HNSCC model and data from the Ba/F3 and MCF10A models, respectively. The agreement between the two datasets was assessed by Kendall's tau correlation coefficient as indicated in the table.

Supplementary Figure 3

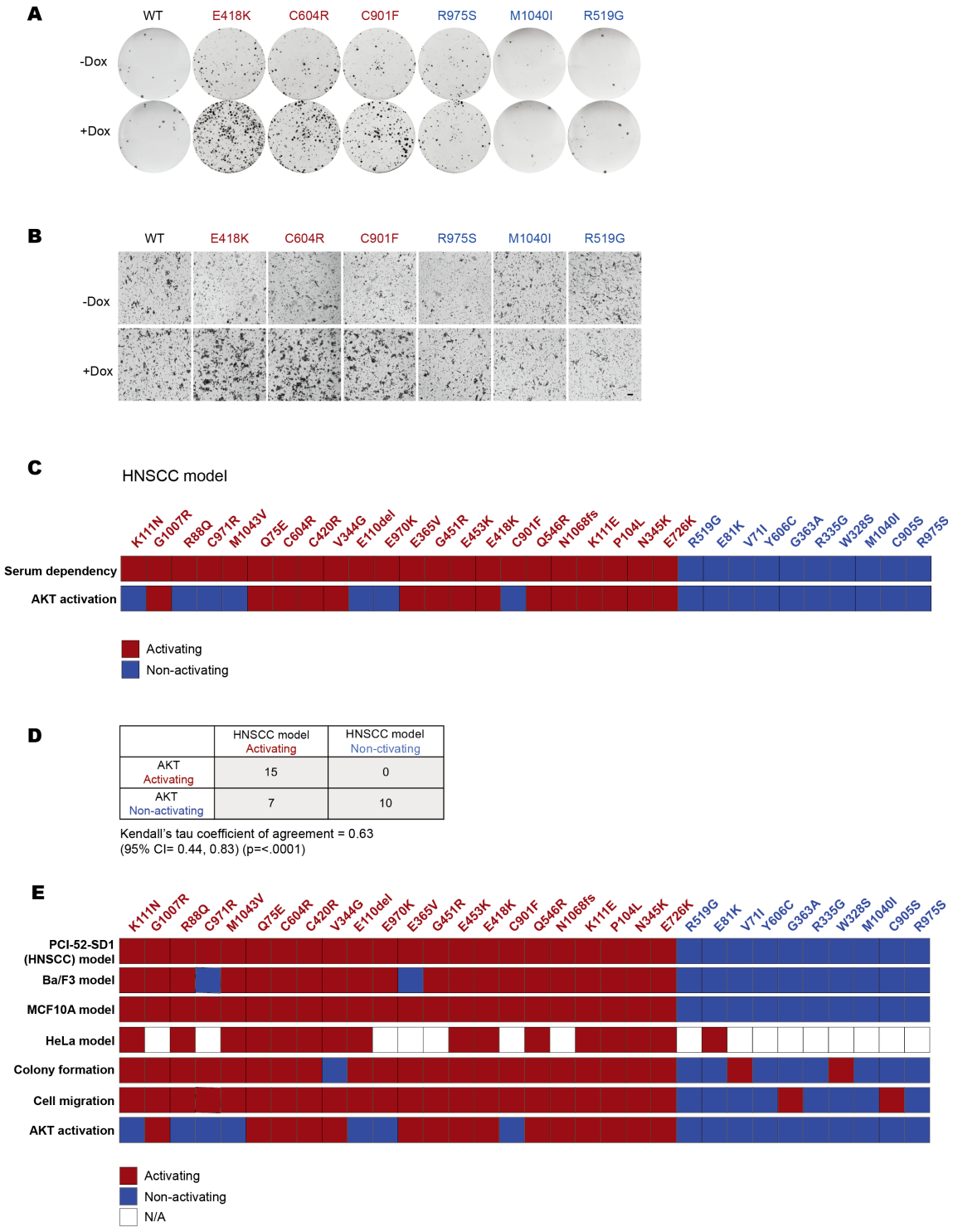

Colony formation and migratory phenotypes of activating and non-activating non-canonical *PIK3CA* mutations

(**A**) Colony formation images of isogenic PCI-52-SD1 HNSCC cells expressing WT *PIK3CA* or the indicated representative activating and non-activating, non-canonical mutants. Cells were cultured in the absence or presence of Dox (1 μg/mL) and incubated for 3 weeks, followed by crystal violet staining. The experiment was repeated twice with similar results. (**B**) Representative cell migration images of cells expressing activating and non-activating *PIK3CA* mutations. Cells were applied to Boyden chambers and incubated for 48 h in the absence or presence of Dox, followed by crystal violet staining. Images were taken from bottom side of the transmembrane chambers. Scale bar, 250 μm. The experiment was repeated twice with similar results. (**C**) Alignment between data from serum-dependence assays and assessments of AKT activation in the isogenic HNSCC cells. The AKT activation was evaluated by immunoblotting to assess the ratio of pAKT (S473)/(total AKT). Mutations were assigned as ‘‘activating’’ if the mutations exhibited an activity higher than WT *PIK3CA*, otherwise the mutations were annotated as ‘‘non-activating’’. (**D**) Correlation analysis between findings from serum-dependence assays and AKT activation assessments in HNSCC models. The agreement between the two datasets was assessed by Kendall’s tau correlation coefficient as indicated in the table. (**E**) Heatmap summarizing activation status and oncogenic phenotype of each HNSCC-associated non-canonical *PIK3CA* mutation across 4 distinct cellular platforms and 2 phenotypic assays and biochemical evaluation of AKT phosphorylation.

Supplementary Figure 4

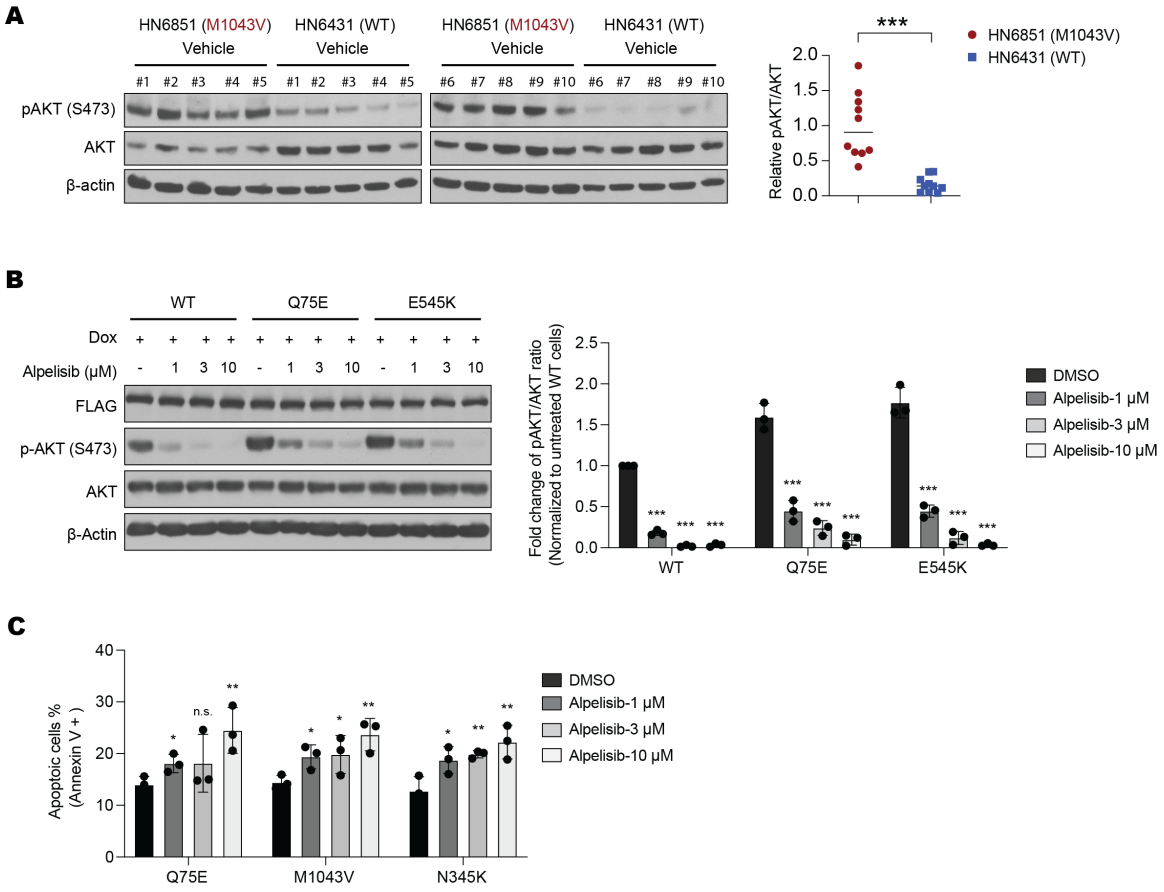

Response to alpelisib in HNSCC preclinical models expressing non-canonical *PIK3CA* mutations

(**A**) Immunoblot analysis of AKT activation in the vehicle treated PDX tumors. Tumor samples were collected at 3 h after the last dosing. AKT activation was detected by the phosphorylation of AKT S473. β-actin, loading control. The fold change in the ratio pAKT/(total AKT) in the HN6851 PDX tumors was quantified by densitometry and normalized to the mean value in the HN6431 PDX tumors. ***p < 0.001 for Student's pairwise t-test. (**B**) Immunoblot analysis of AKT activation in the isogenic PCI-52-SD1 cells expressing WT or mutant *PIK3CA*. Cells in the presence of Dox (1 ug/mL) were treated alpelisib at 1 μM, 3 μM and 10 μM for 3 h before harvesting. AKT activation was detected by phosphorylation of S473. β-actin, loading control. The experiment was repeated three times with similar results. The fold change of the ratio of pAKT/(total AKT)

was quantified by densitometry and normalized to the untreated WT cells. (**C**) Cell apoptosis assays. PCI-52-SD1 cells in the presence of Dox (1 ug/mL) were treated with alpelisib at 1 μM, 3 μM and 10 μM for 72 h. The percentage of apoptosis was determined by flow cytometry using Annexin V staining. The experiment was repeated three times with similar results. Columns represent the mean ± sd. **$p < 0.01$, *$p < 0.1$, n.s. ≥ 0.05 for Student's pairwise t-test.

Supplementary Table 1. Next generation sequencing results of the index patient's tumor

Next generation sequencing of the index patient's recurrent tumor for 244 genes known to be somatically altered in HNSCC revealed a non-canonical *PIK3CA* mutation.

SNV & indel							
Chromosome	**Start**	**End**	**Symbol**	**Amino_acid**	**Exonic_function**	**Cosmic**	**ICGC**
4	153247366	153247366	FBXW7	p.R361Q, p.R399Q, p.R479Q	nonsynonymous SNV	41	12
3	30732970	30732970	TGFBR2	p.R553H, p.R528H	nonsynonymous SNV	4	3
3	142168444	142168444	ATR	p.A2588S	nonsynonymous SNV	0	0
3	178916836	178916836	PIK3CA	p.Q75E	nonsynonymous SNV	1	1

CNV						
Tool	**Sample ID**	**Chromosome**	**Start**	**End**	**Gene symbol**	**CN**
CNVkit	27-S031	chr3	181430138	181579744	SOX2	14

mRNA expression			
Gene Name	**UP TOP 5**	**Gene Name**	**DOWN TOP 5**
CXCL9	7.21	JCHAIN	-607.27
CXCL10	3.95	CXCR5	-49.64
BST2	3.47	CD27	-33.42
CXCL13	2.54	BTN1A1	-21.48
HPRT1	2.14	LY9	-14.7

NGS panel (244 genes known to be somatically altered in HNSCC)

ABL1	ABL2	AKT1	AKT2	AKT3	APC	AR
ATM	ATR	ATRX	AURKA	AURKB	AXL	BAP1
BRCA2	BRD3	BRD4	BRD7	BUB1	CASP8	CBL
CDH9	CDK12	CDK4	CDK6	CDK8	CDKN1B	CDKN2A
CHD4	CHD5	CHD7	CHEK1	CHEK2	CREBBP	CRKL
CUL3	DACH1	DAXX	DDR2	DNMT1	DNMT3A	DNMT3B
EPHA2	EPHA3	EPHA4	EPHA5	EPHA7	EPHB1	EPHB4
FAM123B	FAT1	FAT2	FAT3	FAT4	FBN2	FBXW7
GATA1	GATA2	GATA3	GNA11	GNA13	GNAQ	GNAS
HDAC7A	HDAC9	HRAS	IDH1	IDH2	IGF1R	IKBKE
KDM5A	KDM5C	KDM6A	KDR	KEAP1	KIT	KLHL1
LAMC2	MAP2K1	MAP2K2	MAP2K4	MAP3K1	MAP3K8	MAP3K9
MLH1	MLL1	MLL2	MLL3	MTOR	MYC	MYCL1
NOTCH1	NOTCH2	NPM1	NRAS	NSD1	PAK3	PAK5(PAK7)
PIK3C2G	PIK3C3	PIK3CA	PIK3CB	PIK3CD	PIK3CG	PIK3R1
PRB2	PRKCI	PTCH1	PTEN	PTK2B	PTPN11	PTPRD

RELN	RHOA	RICTOR	RIT1	RPS6KA1	RPTOR	SETD2
SMARCA4	SMARCA4	SMARCB1	SMO	SOCS1	SOX10	SOX2
TET2	TGFBR2	TOP1	TP53	TP63	TRIO	TSC1
ARAF	ARID1A	ARID2	ASH1L	ASXL1	ASXL3	TSC2
BARD1	BIRC3	BIRC6	BLM	BRAF	BRCA1	VHL
CCND1	CCND2	CCND3	CCNE1	CDH1	CDH10	WHSC1L1
CDKN2B	CDKN2C	CEBPA	CEP350	CFTR	CHD2	
CTNNA1	CTNNA2	CTNNB1	CTNND2	CTSK	CTTN	
DOT1L	DUSP27	EGFR	EP300	EPCAM	EPHA1	
ERBB	ERBB2	ERBB3	ERBB4	ERG	EZH2	
FES	FGFR1	FGFR2	FGFR3	FGFR4	FOXP1	
GPR98	HDAC1	HDAC2	HDAC3	HDAC5	HDAC6	
IL7R	ITGB1	ITGB3	JAK1	JAK2	JAK3	
KLHL6	KMT2D	KRAS	LAMA2	LAMA3	LAMB3	
MAPK1	MAPK9	MBD1	MBD2	MDM4	MET	
MYCN	NF1	NF2	NFE2L2	NFKBIA	NKX2-1	
PBRM1	PDGFRA	PDGFRB	PDK1	PIK3C2A	PIK3C2B	
PIK3R2	PIK3R3	PIK3R6	PPFIA2	PPP2R1A	PRB1	
RAC1	RAD50	RAD51	RAF1	RASSF1A	RB1	
SIRT1	SIRT2	SMAD2	SMAD3	SMAD4	SMARCA2	
SRC	STAT3	STAT4	STK11	STYK1	TERT	

73

Supplementary Table 2. Targeted sequencing results of PCI-52 cells

Gene_Name	Chromosome	snpEff.EFF	Effefct_Impact	Functional _Class	Codon _Change	Amino_Acid _change
PDGFRB	5	NON_SYNONYMOUS_CODING	MODERATE	MISSENSE	aCg/aTg	T464M
MSH6	2	NON_SYNONYMOUS_CODING	MODERATE	MISSENSE	aTa/aCa	I967T
RB1	13	NON_SYNONYMOUS_CODING	MODERATE	MISSENSE	Gcg/Tcg	A18S
PRKCG	19	NON_SYNONYMOUS_CODING	MODERATE	MISSENSE	cGc/cAc	R252H
PDGFRA	4	NON_SYNONYMOUS_CODING	MODERATE	MISSENSE	Atc/Gtc	I539V
PTCH1	9	INTRON_MODIFIER	LOW	-	-	-
ATM	11	NON_SYNONYMOUS_CODING	MODERATE	MISSENSE	Atg/Gtg	M963V
APC	5	NON_SYNONYMOUS_CODING	MODERATE	MISSENSE	Aat/Cat	N2726H
CSMD3	8	NON_SYNONYMOUS_CODING	MODERATE	MISSENSE	Agt/Cgt	S2282R
TP53	17	CODON_CHANGE_PLUS_CODON_DELETION	MODERATE	-	aactacatg/atg	NYM103M
BIRC2	11	FRAME_SHIFT	HIGH	-	-	-

Supplementary Table 3. Functional characterization of all 32 non-canonical *PIK3CA* mutations in cytokine/growth factor-dependent Ba/F3 and MCF10A cell line models

Cells were transfected with WT *PIK3CA* or indicated *PIK3CA* mutants, and then cultured for 4 weeks and harvested for CellTiter-Glo viability assays. The relative cell viability for each mutant is calculated by the normalization to a range of 1 to 100, when WT *PIK3CA* is 1 and the positive control (a canonical mutant *PIK3CA* H1047R) is 100. Mutations were not accessed in the same one experiment and the statistical comparison between WT and mutant (t-test) was done within the same experiment.

BaF3 cell model

Experiment Number	AA_Change	The relative cell viability Average	SD	p-value	Annotation
B01	V71I	0.55	0.05	0.528	Non-activating
B02	W328S	1.35	0.22	0.415	Non-activating
B03	C905S	2.35	1.44	0.383	Non-activating
B03	R519G	2.03	0.03	0.448	Non-activating
B04	E970K	32.12	3.53	0.000	Activating
B04	M1040I	-1.53	2.21	0.370	Non-activating
B05	E418K	10.64	1.40	0.015	Activating
B05	Y606C	-0.43	0.34	0.567	Non-activating
B05	R335G	1.58	1.24	0.815	Non-activating
B06	Q75E	81.29	9.63	0.026	Activating
B07	E726K	115.68	30.96	<0.0001	Activating
B07	M1043V	159.91	1.89	<0.0001	Activating
B07	Q546R	163.99	1.05	<0.0001	Activating
B08	C420R	94.38	24.07	0.002	Activating
B09	C604R	45.65	17.16	0.000	Activating
B09	R975S	2.75	4.73	0.616	Non-activating
B09	C901F	41.99	1.38	<0.0001	Activating
B10	G451R	20.50	9.02	0.018	Activating
B10	E365V	1.15	0.61	0.978	Non-activating
B11	N1068fs	37.77	1.96	0.001	Activating
B11	G363A	1.96	0.22	0.060	Non-activating
B11	C971R	1.38	0.27	0.293	Non-activating
B12	K111N	12.11	6.66	0.001	Activating
B12	R88Q	11.89	8.94	0.003	Activating
B12	N345K	59.74	6.55	<0.0001	Activating
B12	E453K	43.14	19.67	<0.0001	Activating
B12	P104L	13.19	2.80	<0.0001	Activating
B12	E110del	49.62	12.54	<0.0001	Activating
B13	V344G	44.61	2.86	0.002	Activating

B13	G1007R	24.11	1.56	0.003	Activating
B13	K111E	19.47	1.87	0.006	Activating

85 **MCF10A cell model**

Experiment Number	AA_Change	The relative cell viability Average	SD	p-value	Annotation
M01	V71I	-8.62	1.68	0.1596	Non-activating
M02	W328S	10.60	4.47	0.2012	Non-activating
M03	R519G	-3.38	7.70	0.4436	Non-activating
M03	C905S	3.04	2.66	0.6444	Non-activating
M04	E970K	38.47	0.04	0.0206	Activating
M04	M1040I	-26.69	4.56	0.0622	Non-activating
M05	E418K	93.84	15.84	0.0126	Activating
M05	Y606C	-26.38	10.52	0.1524	Non-activating
M05	R335G	7.91	34.14	0.4624	Non-activating
M06	Q75E	60.38	18.24	0.0084	Activating
M07	E726K	79.20	13.45	<0.0001	Activating
M07	M1043V	87.21	22.59	<0.0001	Activating
M07	Q546R	115.34	22.98	<0.0001	Activating
M08	C420R	73.89	19.78	0.0007	Activating
M09	C901F	105.57	31.29	0.0002	Activating
M09	C604R	94.19	35.85	0.0005	Activating
M09	R975S	-6.55	0.02	0.3164	Non-activating
M10	E365V	24.57	7.57	<0.0001	Activating
M10	G451R	67.80	5.79	<0.0001	Activating
M11	N1068fs	21.73	3.23	0.0231	Activating
M11	C971R	18.00	2.29	0.0256	Activating
M11	G363A	-1.06	0.27	0.4579	Non-activating
M12	K111N	7.60	1.41	0.0014	Activating
M12	E110del	21.69	2.56	<0.0001	Activating
M12	E453K	17.77	3.23	<0.0001	Activating
M12	N345K	87.62	8.92	<0.0001	Activating
M12	P104L	14.81	0.57	<0.0001	Activating
M12	R88Q	21.60	3.66	<0.0001	Activating
M13	K111E	122.33	11.29	0.0047	Activating
M13	G1007R	81.82	7.79	0.0055	Activating
M13	V344G	70.60	12.08	0.0159	Activating

86

Supplementary Table 4. Whole exome sequencing results of HNSCC PDX models

HN6851 (*PIK3CA* M1043V)

Hugo_Symbol	Chromosome	Start_position	End_position	Variant_Classification	cDNA_Change	Protein_Change	i_tumor_f
CATSPER4	1	26524456	26524456	Missense_Mutation	c.566G>A	p.R189H	0.125
CCDC24	1	44457994	44457994	Missense_Mutation	c.237C>G	p.D79E	0.117021
STXBP3	1	109319034	109319034	Missense_Mutation	c.673A>T	p.S225C	0.140351
KIF21B	1	200974705	200974705	Missense_Mutation	c.565G>A	p.V189I	0.098485
TMCC2	1	205211075	205211075	Missense_Mutation	c.650G>A	p.R217H	0.15625
KLHDC8A	1	205308535	205308535	Missense_Mutation	c.544G>A	p.G182R	0.076923
OR2T29	1	248722108	248722108	Missense_Mutation	c.667G>A	p.V223I	1
OR51E1	11	4674565	4674565	Missense_Mutation	c.809G>A	p.R270H	0.092391
OR56B4	11	6129261	6129261	Missense_Mutation	c.253C>T	p.P85S	0.095238
SLC17A6	11	22363183	22363183	Missense_Mutation	c.196G>A	p.G66S	0.106195
OR4S2	11	55419037	55419037	Missense_Mutation	c.658C>A	p.L220I	0.103825
BSCL2	11	62459926	62459926	Missense_Mutation	c.593C>T	p.A198V	0.081633
LTBP3	11	65320345	65320345	Missense_Mutation	c.1172G>A	p.R391H	0.095808
TBX10	11	67399247	67399247	Missense_Mutation	c.987C>G	p.S329R	0.181818
TSKU	11	76507325	76507325	Missense_Mutation	c.665C>T	p.P222L	0.072917
TYR	11	88924442	88924442	Missense_Mutation	c.892C>T	p.R298W	0.122995
LOC100288778	12	90650	90650	Missense_Mutation	c.656A>G	p.H219R	0.136364
Unknown	12	92000	92000	Missense_Mutation	c.310T>A	p.L104M	0.185185
Unknown	12	92018	92018	Missense_Mutation	c.292A>G	p.S98G	0.09375
CD163L1	12	7551154	7551154	Missense_Mutation	c.1435G>T	p.V479F	0.068571
A2M	12	9265958	9265958	Missense_Mutation	c.268G>A	p.A90T	0.082474
DDX11	12	31237922	31237922	Missense_Mutation	c.500G>C	p.R167T	0.172414
NUP107	12	69135678	69135678	Missense_Mutation	c.2588C>T	p.T863M	0.122807
E2F7	12	77417806	77417806	Missense_Mutation	c.2725G>A	p.G909S	0.11236
PLEKHG7	12	93157951	93157951	Missense_Mutation	c.915T>G	p.I305M	0.081633
TTC7B	14	91252634	91252634	Missense_Mutation	c.160G>A	p.E54K	0.052632
ATPBD4	15	35834681	35834681	Missense_Mutation	c.51G>A	p.M17I	0.129032
TBC1D2B	15	78290635	78290635	Missense_Mutation	c.2759G>A	p.R920Q	0.111111
CLEC18C	16	70218491	70218491	Missense_Mutation	c.1079T>C	p.I360T	1
TP53	17	7578393	7578393	Missense_Mutation	c.537T>G	p.H179Q	0.152174
PRPSAP2	17	18793162	18793162	Missense_Mutation	c.556G>T	p.V186L	0.140741
MYO1D	17	31048183	31048183	Missense_Mutation	c.1771A>C	p.K591Q	0.09596
DCC	18	51013172	51013172	Missense_Mutation	c.3742G>A	p.V1248M	0.13369
FCGBP	19	40363188	40363188	Missense_Mutation	c.14882G>A	p.R4961Q	0.072165
CCDC8	19	46915802	46915802	Missense_Mutation	c.266C>T	p.P89L	0.106742
VIT	2	36970284	36970284	Missense_Mutation	c.160A>G	p.I54V	0.125
MAP1D	2	172928445	172928445	Missense_Mutation	c.205A>C	p.K69Q	0.145161

TTC30B	2	178416842	178416842	Missense_Mutation	c.650G>A	p.R217H	0.059211
TTN	2	179636076	179636076	Missense_Mutation	c.7978C>T	p.P2660S	0.08209
CXCR2P1	2	218925687	218925687	Missense_Mutation	c.34C>T	p.R12C	0.076923
ALPP	2	233246399	233246399	Missense_Mutation	c.1502C>G	p.P501R	0.113636
OVOL2	20	18022218	18022218	Missense_Mutation	c.471C>G	p.N157K	0.079208
ARFGAP1	20	61917793	61917793	Missense_Mutation	c.910A>T	p.S304C	0.121622
CHEK2	22	29091840	29091840	Missense_Mutation	c.1117A>G	p.K373E	0.043478
TRIM42	3	140397391	140397391	Missense_Mutation	c.320G>A	p.R107H	0.077778
PIK3CA	3	178952072	178952072	Missense_Mutation	c.3127A>G	p.M1043V	0.128492
ZNF141	4	367455	367455	Missense_Mutation	c.1229G>A	p.R410Q	0.070588
SPATA5	4	123857311	123857311	Missense_Mutation	c.1334G>A	p.R445Q	0.126437
SDHAP3	5	1593264	1593264	Missense_Mutation	c.196G>A	p.A66T	0.134615
PSD2	5	139221863	139221863	Missense_Mutation	c.2120G>A	p.R707H	0.075269
MUC17	7	100683801	100683801	Missense_Mutation	c.9104G>A	p.G3035D	0.136364
NUP214	9	134025736	134025736	Missense_Mutation	c.2066C>T	p.A689V	0.094595
TUBBP5	9	141071154	141071154	Missense_Mutation	c.557T>C	p.V186A	0.096386
TUBBP5	9	141071195	141071195	Missense_Mutation	c.598C>T	p.P200S	0.149123
XPNPEP2	X	128901598	128901598	Missense_Mutation	c.1760C>T	p.T587I	0.166667
MLL4	19	36214821	36214821	Nonsense_Mutation	c.3247C>T	p.R1083*	0.083333
MAP4K1	19	39100635	39100635	Nonsense_Mutation	c.841C>T	p.R281*	0.094891
NAT8B	2	73928312	73928312	Nonsense_Mutation	c.121C>T	p.R41*	0.080214
NBPF14	1	148004525	148004525	3'UTR			0.102439
FAM22A	10	88994492	88994492	3'UTR			1
FAM22A	10	88994534	88994534	3'UTR			1
CXADRP2	15	22015940	22015940	3'UTR			0.138889
FLJ35220	17	78410119	78410119	3'UTR			0.333333
CCRN4L	4	139966663	139966663	3'UTR			0.159091
CYP21A2	6	31975463	31975463	3'UTR			0.102564
FAM46A	6	82459344	82459344	3'UTR			0.108108
Unknown	9	84675669	84675669	3'UTR			0.092784
Unknown	15	102297229	102297229	5'Flank			1
SLCO1B3	12	20968655	20968655	5'UTR			0.25
GOLGA8E	15	23438847	23438847	5'UTR			1
RGPD4	2	108443438	108443438	5'UTR			0.153846
LYPLA2P1	6	33334078	33334078	5'UTR			0.078947
KCNK5	6	39196946	39196946	5'UTR			0.125
MAGEA3	X	151936356	151936356	5'UTR			1
CCDC30	1	43055286	43055286	Intron			0.115385
KIAA0907	1	155884143	155884143	Intron			0.26087
CSTF3	11	33163119	33163119	Intron			0.210526
ITGB7	12	53591255	53591255	Intron			0.084507

Unknown	15	20644688	20644688	Intron			0.137931
CDRT1	17	15502013	15502013	Intron			0.105263
LOC644165	22	25043098	25043098	Intron			0.070423
SERHL2	22	42969919	42969919	Intron			0.103704
CPSF1	8	145620789	145620789	Intron			0.25
LOC642846	12	9458891	9458891	RNA	c.1928A>G		0.157895
LOC374491	13	25144704	25144704	RNA	c.245T>C		0.194444
GOLGA6L5	15	85059998	85059998	RNA	c.81C>T		1
Unknown	16	70268080	70268080	RNA	c.335A>G		0.157895
Unknown	16	70268158	70268158	RNA	c.257T>G		0.148148
Unknown	9	67793910	67793910	RNA	c.1744G>A		1
Unknown	9	135895805	135895805	RNA	c.9G>T		0.090909
VPS13D	1	12516089	12516089	Silent	c.12369G>A	p.T4123T	0.066667
NBPF10	1	145360624	145360624	Silent	c.9474G>A	p.S3158S	0.190476
OR5L2	11	55595474	55595474	Silent	c.780C>T	p.C260C	0.201087
MMAB	12	109996930	109996930	Silent	c.615C>T	p.T205T	0.104348
PCDH9	13	67800215	67800215	Silent	c.2358C>T	p.D786D	0.165775
HDAC5	17	42160973	42160973	Silent	c.2403G>A	p.V801V	0.071429
TTN	2	179486278	179486278	Silent	c.37569C>T	p.N12523N	0.081633
CHRNA4	20	61981485	61981485	Silent	c.1278C>T	p.S426S	0.142857
ATG7	3	11382147	11382147	Silent	c.918G>A	p.K306K	0.098901
LRRC31	3	169572686	169572686	Silent	c.906G>A	p.S302S	0.1125
SDHAP2	3	195410640	195410640	Silent	c.537T>C	p.Y179Y	0.073171
C5orf49	5	7850994	7850994	Silent	c.141G>A	p.P47P	0.086957
WASF1	6	110424661	110424661	Silent	c.813A>G	p.V271V	0.098958
SYNJ2	6	158454679	158454679	Silent	c.678C>T	p.D226D	0.054645
ALG2	9	101980369	101980369	Silent	c.1098G>A	p.P366P	0.054348
CACNA1F	X	49084827	49084827	Silent	c.900C>T	p.R300R	0.093023

89

HN6431 (*PIK3CA* WT)

Hugo_Symbol	Chromosome	Start_position	End_position	Variant_Classification	cDNA_Change	Protein_Change	i_tumor_f
PRAMEF22	1	13035545	13035545	Missense_Mutation	c.3G>C	p.M1I	1
AKR7A3	1	19612764	19612764	Missense_Mutation	c.317G>A	p.R106Q	0.115183
PTP4A2	1	32377362	32377362	Missense_Mutation	c.255A>T	p.L85F	0.181287
SLFNL1	1	41483450	41483450	Missense_Mutation	c.814C>T	p.R272C	0.147929
PPCS	1	42922346	42922346	Missense_Mutation	c.110T>G	p.V37G	0.236842
LEPR	1	66067341	66067341	Missense_Mutation	c.1261C>T	p.R421C	0.163462
CSF1	1	110466000	110466000	Missense_Mutation	c.757C>T	p.P253S	0.13245
ANXA9	1	150956535	150956535	Missense_Mutation	c.257G>A	p.R86H	0.073171
ASH1L	1	155450764	155450764	Missense_Mutation	c.1897G>T	p.V633L	0.162651
SLAMF1	1	160607290	160607290	Missense_Mutation	c.106C>A	p.L36I	0.117647
RC3H1	1	173952657	173952657	Missense_Mutation	c.491G>A	p.R164Q	0.100719
FMN2	1	240371009	240371009	Missense_Mutation	c.2897T>C	p.L966P	0.103093
PARG	10	51093329	51093329	Missense_Mutation	c.1750G>A	p.A584T	0.03937
NCOA4	10	51580587	51580587	Missense_Mutation	c.173G>A	p.R58H	0.12
HRAS	11	534289	534289	Missense_Mutation	c.34G>A	p.G12S	0.144144
MUC5B	11	1269115	1269115	Missense_Mutation	c.12589G>A	p.G4197S	0.110236
OR4A5	11	51411686	51411686	Missense_Mutation	c.710G>T	p.C237F	0.160221
OR5W2	11	55681455	55681455	Missense_Mutation	c.604G>A	p.V202I	0.150289
SAPS3	11	68312482	68312482	Missense_Mutation	c.404A>T	p.K135I	0.128378
KBTBD3	11	105923623	105923623	Missense_Mutation	c.1793A>C	p.Q598P	0.116279
TMEM132B	12	126138806	126138806	Missense_Mutation	c.2787A>T	p.K929N	0.134715
CDK8	13	26959417	26959417	Missense_Mutation	c.584T>C	p.V195A	0.141593
RNF219	13	79189852	79189852	Missense_Mutation	c.2044C>G	p.L682V	0.233503
SLITRK5	13	88328944	88328944	Missense_Mutation	c.1301G>A	p.G434E	0.125874
JUB	14	23444276	23444276	Missense_Mutation	c.1277G>A	p.C426Y	0.105263
MKRN3	15	23811363	23811363	Missense_Mutation	c.434C>T	p.T145M	0.145161
IQCH	15	67709344	67709344	Missense_Mutation	c.2173C>T	p.R725W	0.128713
Unknown	16	28354457	28354457	Missense_Mutation	c.695C>T	p.P232L	0.09375
PRSS53	16	31097782	31097782	Missense_Mutation	c.539G>A	p.R180H	0.15
CSF3	17	38172072	38172072	Missense_Mutation	c.169G>A	p.D57N	0.139535
KRTAP4-7	17	39240627	39240627	Missense_Mutation	c.169T>C	p.S57P	0.099415
CUEDC1	17	55946537	55946537	Missense_Mutation	c.886C>T	p.P296S	0.135802
BCAS3	17	58967129	58967129	Missense_Mutation	c.735C>G	p.N245K	0.166667
C17orf28	17	72948430	72948430	Missense_Mutation	c.2078C>T	p.P693L	0.132075
TMEM200C	18	5891942	5891942	Missense_Mutation	c.121G>T	p.V41L	0.106667
ANKRD30B	18	14851970	14851970	Missense_Mutation	c.3670T>A	p.Y1224N	0.131579
DCC	18	50278661	50278661	Missense_Mutation	c.329C>T	p.P110L	0.12426
POLRMT	19	622886	622886	Missense_Mutation	c.1390C>T	p.R464W	0.487179
MUC16	19	9003333	9003333	Missense_Mutation	c.40102G>A	p.V13368I	0.418919

DNMT1	19	10265093	10265093	Missense_Mutation	c.1847C>T	p.T616M	0.401042
SMARCA4	19	11141427	11141427	Missense_Mutation	c.3404G>A	p.R1135Q	0.290323
ZNF233	19	44778750	44778750	Missense_Mutation	c.1937A>C	p.K646T	0.394444
VSTM1	19	54544333	54544333	Missense_Mutation	c.593C>T	p.T198M	0.459459
MYT1L	2	1843078	1843078	Missense_Mutation	c.2923G>A	p.A975T	0.162921
CTNNA2	2	79971609	79971609	Missense_Mutation	c.199G>A	p.A67T	0.135922
PPIG	2	170489726	170489726	Missense_Mutation	c.986C>A	p.S329Y	0.13913
TTN	2	179528398	179528398	Missense_Mutation	c.926C>T	p.A309V	0.177885
TTN	2	179605415	179605415	Missense_Mutation	c.12032A>G	p.E4011G	0.113514
HDAC4	2	240003803	240003803	Missense_Mutation	c.2632G>T	p.D878Y	0.108247
SEC61A1	3	127786268	127786268	Missense_Mutation	c.980C>T	p.T327M	0.205556
SPATA16	3	172835185	172835185	Missense_Mutation	c.337C>A	p.P113T	0.154867
WDR1	4	10083028	10083028	Missense_Mutation	c.1237G>A	p.V413I	0.16
WDR19	4	39245929	39245929	Missense_Mutation	c.2483G>A	p.R828H	0.147059
PCDH10	4	134071698	134071698	Missense_Mutation	c.403G>A	p.A135T	0.1
GUSBP1	5	21491446	21491446	Missense_Mutation	c.192G>T	p.Q64H	0.209302
C5orf34	5	43506091	43506091	Missense_Mutation	c.691C>T	p.H231Y	0.109375
GRAMD3	5	125813462	125813462	Missense_Mutation	c.565G>T	p.A189S	0.137363
CSF1R	5	149459795	149459795	Missense_Mutation	c.412G>A	p.V138I	0.132743
ADAMTS2	5	178562959	178562959	Missense_Mutation	c.2036G>A	p.R679H	0.070423
HIST1H3H	6	27777869	27777869	Missense_Mutation	c.18G>T	p.Q6H	0.157609
DNAH8	6	38775449	38775449	Missense_Mutation	c.2563C>T	p.R855W	0.126437
C6orf150	6	74135219	74135219	Missense_Mutation	c.1300T>C	p.S434P	0.207317
C6orf191	6	130166922	130166922	Missense_Mutation	c.109G>A	p.V37M	0.132075
PCLO	7	82764239	82764239	Missense_Mutation	c.2627C>T	p.P876L	0.110553
MUC17	7	100676343	100676343	Missense_Mutation	c.1646G>A	p.S549N	0.246231
ZNF282	7	148907754	148907754	Missense_Mutation	c.910C>T	p.R304W	0.151515
CSMD1	8	3267060	3267060	Missense_Mutation	c.1632C>G	p.F544L	0.222222
DLC1	8	12958063	12958063	Missense_Mutation	c.1783C>T	p.R595C	0.151163
LZTS1	8	20107511	20107511	Missense_Mutation	c.1513G>A	p.E505K	0.171123
KCNQ3	8	133196535	133196535	Missense_Mutation	c.557G>T	p.G186V	0.116402
C8orf73	8	144650361	144650361	Missense_Mutation	c.1715T>C	p.V572A	0.142857
FREM1	9	14808085	14808085	Missense_Mutation	c.2941G>C	p.V981L	0.173653
FAM75A2	9	39357770	39357770	Missense_Mutation	c.263C>G	p.P88R	1
FAM189A2	9	72006659	72006659	Missense_Mutation	c.1292G>A	p.R431Q	0.131148
IARS	9	95004436	95004436	Missense_Mutation	c.3177G>C	p.Q1059H	0.136095
NLGN3	X	70367763	70367763	Missense_Mutation	c.164G>A	p.R55Q	0.291667
ARHGAP11B	15	30938316	30938316	Splice_Site	c.1127_splice		0.080645
C20orf194	20	3295768	3295768	Splice_Site	c.1591_splice	p.G531_splice	0.121212
C21orf99	21	14437495	14437495	Splice_Site	c.2166_splice		0.259259
ZMAT4	8	40554763	40554763	Splice_Site	c.349_splice	p.A117_splice	0.109948

TP73	1	3599708	3599708	Silent	c.150C>T	p.D50D	0.122995
C1orf175	1	55175809	55175809	Silent	c.3921C>T	p.R1307R	0.217391
EPHX4	1	92528795	92528795	Silent	c.1041C>T	p.N347N	0.16092
KCNA2	1	111146157	111146157	Silent	c.1248C>T	p.F416F	0.085427
SMNDC1	10	112055010	112055010	Silent	c.555C>T	p.A185A	0.072581
TMEM216	11	61161357	61161357	Silent	c.117T>G	p.G39G	0.173913
GRIN2B	12	13716227	13716227	Silent	c.3945C>T	p.A1315A	0.162921
SOX5	12	23696176	23696176	Silent	c.1740C>T	p.D580D	0.099476
WSCD2	12	108620880	108620880	Silent	c.918G>A	p.A306A	0.125683
TBX3	12	115112081	115112081	Silent	c.1659C>T	p.V553V	0.384615
ZNF592	15	85345396	85345396	Silent	c.3576G>A	p.A1192A	0.170213
MVP	16	29853138	29853138	Silent	c.1413C>T	p.Y471Y	0.089888
ITGA2B	17	42463013	42463013	Silent	c.480C>T	p.S160S	0.0625
SLC17A9	20	61597910	61597910	Silent	c.1095G>A	p.P365P	0.162162
IFNGR2	21	34809233	34809233	Silent	c.978G>A	p.P326P	0.12
NBEAL2	3	47046506	47046506	Silent	c.6339C>T	p.L2113L	0.172414
FXR1	3	180688142	180688142	Silent	c.1599G>T	p.G533G	0.119497
GABRB1	4	47034444	47034444	Silent	c.183C>T	p.V61V	0.125
DDX60L	4	169315637	169315637	Silent	c.3789C>T	p.L1263L	0.15942
GRM1	6	146350827	146350827	Silent	c.174G>A	p.P58P	0.149068
LRRC17	7	102580025	102580025	Silent	c.921C>T	p.I307I	0.116402
CYP4Z2P	1	47325212	47325212	RNA	c.1356C>T		0.291667
LOC653113	12	8384474	8384474	RNA	c.1314G>A		0.136842
ADAM6	14	106054585	106054585	RNA	c.62901G>T		0.110169
Unknown	15	28900606	28900606	RNA	c.537C>T		0.203704
GGT8P	2	91969071	91969071	RNA	c.1402T>C		0.108696
Unknown	21	15278157	15278157	RNA	c.5G>A		0.157895
Unknown	21	15278172	15278172	RNA	c.20T>C		0.190476
LOC348926	4	3948744	3948744	RNA	c.1591C>T		0.181818
SFRS15	21	33065709	33065709	Nonsense_Mutation	c.1411C>T	p.R471*	0.151079
SFRS15	21	33068512	33068512	Nonsense_Mutation	c.982C>T	p.Q328*	0.162304
ACSL6	5	131329909	131329909	Nonsense_Mutation	c.10C>T	p.Q4*	0.137931
TIE1	1	43772707	43772707	Intron			0.128571
PDE4DIP	1	144863505	144863505	Intron			0.086957
NBPF15	1	148574712	148574712	Intron			1
CLEC7A	12	10279991	10279991	Intron			0.139535
GOLGA6L10	15	82932487	82932487	Intron			1
GOLGA6L10	15	82932518	82932518	Intron			1
USP31	16	23085242	23085242	Intron			0.23913
SPON2	4	1164130	1164130	Intron			0.133333
Unknown	7	142206745	142206745	Intron			0.12766

GALNT11	7	151800369	151800369	Intron			0.123077
ZBED1	X	2418415	2418415	Intron			0.3
FAM104B	X	55172471	55172471	Intron			0.24
PCGF2	17	36896673	36896673	5'UTR			0.177778
SDHAP1	3	195706728	195706728	5'UTR			0.076923
GYPE	4	144826679	144826679	5'UTR			0.064748
CAMK2A	5	149669266	149669266	5'UTR			0.229167
ATF6B	6	32095996	32095996	5'UTR			0.325581
MRPS10	6	42185632	42185632	5'UTR			0.111111
FOXD4L5	9	70181379	70181379	5'Flank			1
NBPF14	1	148004475	148004475	3'UTR			0.157895
PLA2G4A	1	186957696	186957696	3'UTR			0.19403
GOLGA8G	15	28634298	28634298	3'UTR			1
C17orf97	17	263918	263918	3'UTR			0.147208
GPS2	17	7215990	7215990	3'UTR			0.285714
STRADB	2	202344965	202344965	3'UTR			0.03876
ARF4	3	57557905	57557905	3'UTR			0.166667
SDHAP1	3	195690149	195690149	3'UTR			0.230769
SDHAP1	3	195690163	195690163	3'UTR			0.263158
F13A1	6	6145758	6145758	3'UTR			0.083333
C6orf168	6	99729009	99729009	3'UTR			0.139535
RLIM	X	73802892	73802892	3'UTR			0.076087

91

Supplementary Table 5. Interactions of *PIK3CA* non-canonical mutations across autoinhibited structures of the PI3Kα heterodimer

Mutations are colored in red or blue according to their function (activating vs non-activating, respectively). Interacting residues are colored according to their domains: ABD in yellow, Linkers in light grey, C2 in blue, HD in pink and KD in violet, while the p85 subunit is in dark grey. Interactions involving the protein backbone are denoted with "bb".

Mutation (PIK3CA)	4L23 (PIK3R1)	4L23 (PIK3CA)	4OVV	4OVU	4L1B	4L2Y	5XGI	Interaction
V71I		I69, I102,	I102,	I102,	I69, I102,	I69, I102,	I69, I102,	Hydrophobic network
Q75E		G8, S7 unmodeled	S7	G8	G8, S7 unmodeled	G8, S7 unmodeled	G8, S7 unmodeled	Hydrogen bond
E81K		K111	N/A	N/A	K111	K111	K111	Salt-bridge
R88Q		D746	D746	D746	D746	D746	E39 or D743	Salt-bridge
P104L		I69, F83	I69, F83	I69, F83	I69, F83	I69, F83	I69, F83	Hydrophobic network
E110del		S306	surface	surface	S306	S306	S306	Hydrogen bond/ surface exposed
K111E/N		E81	bb-M304	surface	E81	E81	E81	Salt-bridge/Hydrogen bond/surface exposed
W328S		F486, P487, I492	F486, P487, I492	F486, P487, I492	F486, P487, I492	F486, P487, I492	F486, P487, I492	Hydrophobic network
R335G		surface	surface	surface	surface	surface	surface	Surface exposed
V344G		V346, I354, W383, I406, L422	V346, I354, W383, I406, L422	V346, I354, W383, I406, L422	V346, I354, W383, I406, L422	V346, I354, W383, I406, L422	V346, I354, W383, I406, L422	Hydrophobic network
N345K	N564		N564	N564	N564	N564	N564	Hydrogen bond

G363A		R401	N/A	N/A	R401	R401	R401	Hydrogen bond
E365V		N377	N377	bb-L367, bb-K374	N377	N377	N377	Hydrogen bond
E418K	K575		bb-V409, p110 loop: K410-E417 unmodeled	p110 loop: K410-415A unmodeled	K575	K575	K575	Salt-bridge/ Hydrogen bond
C420R	P568		P568	P568	P568	P568	P568	Van der Waals
E453K	R574		bb-L570	K567	R574	R574	R574	Salt-bridge/ Hydrogen bond
G451R		bb-P449	bb-P449	bb-P449	bb-P449	bb-P449	bb-P449	Hydrogen bond
R519G		surface	unmodeled	N/A	unmodeled	unmodeled	Surface	Surface-exposed/ salt-bridge
Q546R	bb-K382		bb-K382	bb-K382	bb-K382	bb-K382	bb-K382	Hydrogen bond
C604R		I459, L1006, F1016	I459, L1006, F1016	I459, L1006, F1016	I459, L1006, F1016	I459, L1006, F1016	I459, L1006, F1016	Hydrophobic network
Y606C		bb-P566	E600	bb-P566 or E600	bb-P566	bb-P566	bb-P566	Hydrogen bond
E726K		surface	surface	surface	surface	surface	surface	Surface exposed at lipid binding interface
C901F		F897, L929, F954, L956, F960, I964, F980	F897, L929, F954, L956, F960, I964, F980	F897, L929, F954, L956, F960, I964, F980	F897, L929, F954, L956, F960, I964, F980	F897, L929, F954, L956, F960, I964, F980	F897, L929, F954, L956, F960, I964, F980	Hydrophobic network
C905S		V952, L956, F980, C984,	V952, L956, F980, C984,	V952, L956, F980, C984, W1051, M1043	V952, L956, F980, C984, W1051, M1043	V952, L956, F980, C984, W1051, M1043	V952, L956, F980, C984, W1051, M1043	Hydrophobic network

		W1051, M1043	W1051, M1043					
E970K		surface	surface	surface	surface	surface	surface	Surface exposed at lipid binding interface
C971R		surface	surface	surface	surface	surface	surface	Surface exposed at lipid binding interface
R975S		surface	surface	surface	surface	surface	surface	Surface exposed
G1007R		Y641	Y641	Y641	Y641	Y641	Y641	Hydrogen bond
M1040I		surface	surface	surface	surface	surface	surface	Surface exposed
M1043V		C905, V952, F909, F1039, W1051	C905, V952, F909, F1039, W1051	C905, V952, F909, F1039, W1051	C905 V952, F909, F1039, W1051	C905 V952, F909, F1039, W1051	C905 V952, F909, F1039, W1051	Hydrophobic network
N1068fs		unmodeled	unmodeled	unmodeled	unmodeled	unmodeled	unmodeled	N/A

98

99

Supplementary methods

Cell culture

PCI-52-SD1 cell line was obtained by clonal selection of the parental PCI-52 cell line (University of Pittsburgh Cancer Institute) by rounds of graded serum selection. Generation of the serum-dependent PCI-52-SD1 cell line has been previously described(1). Cells were maintained in complete Dulbecco's Modified Eagle's Medium (DMEM) (Corning, 10-013-CM) with 10% fetal bovine serum (FBS) (Gemini, 900-108) and 1% penicillin/streptomycin (Gibco, 15140-122). Cells engineered to express WT or mutant *PIK3CA* were cultured in complete DMEM containing 0.25 μg/mL puromycin. Cells were maintained at 37 ^{o}C and 5% CO_2. Cells were authenticated by the University of California, Berkeley Cell Culture Facility using the Short Tandem Repeat (STR) method and tested for mycoplasma using PCR detection kit (Sigma, MP0035).

Chemicals and antibodies

Puromycin was from InvivoGen (ant-pr-1) and doxycycline from Cayman (24390-14-5). Antibodies recognizing p-AKT S473 (Rabbit mAb, #4060L), AKT (Rabbit mAb, #4685S), GAPDH (Rabbit mAb, 2118L) were from Cell Signaling Technology. Anti-FLAG (Mouse mAb, #F1804) was from Sigma-Aldrich and anti-β-actin (Rabbit polyclonal, #Ab8227) from Abcam. Primary antibodies were diluted 1:1000 for immunoblotting, with the exception of anti-GAPDH and anti-β-actin which were diluted 1:8000. All secondary antibodies, including horseradish peroxidase (HRP)-conjugated goat anti-rabbit IgG, and anti-mouse IgG (Bio-Rad, 170-6515 and 170-6516) were used at 1:5000 dilution.

Serum-dependent growth assay in HNSCC cells

Cells were trypsinized and seeded in triplicate in 12-well plates at $6X10^4$ cells/well. Following a 24-h incubation, cells were treated with doxycycline (1 μg/mL) for 24 h. Cells were then washed twice with phosphate-buffered saline (PBS) and cultured for 72 h in media containing doxycycline

with either normal FBS (10%) or low FBS (1-2%). To assess proliferation, cells were stained with crystal violet, followed by air drying. Crystal violet was eluted with 1 mL sodium citrate solution (200 mM sodium citrate:100% ethanol=1:1) per well. Eluentswere transferred to 96-well plates, and the absorbance was measured with an Epoch plate reader (BioTek, EPOCH) at 590 nm (A590) to determine cell growth. The percentage of proliferating cells was calculated by comparison of the A590 reading from cells grown in normal FBS versus low FBS.

Immunoblot analysis

Cells were collected and lysed using RIPA, supplemented with protease and phosphatase inhibitors, followed by sonication and centrifugation at 13,000 rpm for 10 min at 4^{o}C. Protein concentrations were determined by Bradford assay (Bio-Rad, 500-0006). Proteins were subjected to SDS-PAGE, transferred to PVDF membranes and blocked for 1 h at room temperature with 5% milk in TBST. Blotting was performed with primary antibodies at 4°C overnight. After washing with TBST three times for 30 min in total, membranes were incubated for 1 h at room temperature with horseradish peroxidase-conjugated anti-rabbit IgG or anti-mouse IgG antibodies. Membranes were then washed with TBST three times for 30 min in total, and the antigen-antibody reaction was visualized with ECL western blotting luminol reagent (Santa Cruz Biotechnology, sc-2048).

Cell migration assay

Cells were trypsinized and seeded at 8X10^{4} cells in 100 µL of serum-free DMEM containing doxycycline (1 µg/mL) into the upper chamber of migration plates with 8 µm pores (Corning, 353097). The lower chamber contained 600 µL of complete DMEM with 10% FBS and doxycycline (1 µg/mL). After 48 h, the media and remaining non-migratory cells in the inserts were removed and the inserts were placed into a new 24-well plate. Cells were stained with crystal violet in 70% ethanol (600 µL/well), as well as 100 µL in the upper insert. After 15 min, the crystal violet

in the internal inserts was removed using cotton tips, followed by washing with distilled water several times. Inserts were air dried and imaged, followed by quantification using ImageJ software.

Colony formation assay

Cells were detached with trypsin and resuspended as single cells (determined by microscopy). 2,000 cells/well were seeded in 6-well plates in triplicate with or without doxycycline (1μg/mL) and grown for 21 days. The cells were then fixed with 4% paraformaldehyde and stained with 0.1% crystal violet stain for 10 min. Following rinsing with distilled water, colonies were imaged and quantified using ImageJ software.

Apoptosis assay

Cells were trypsinized and seeded at $4X10^5$ cells in complete DMEM containing doxycycline (1 μg/mL), then treated for 72 h with alpelisib. Treated cells were washed with cold PBS resuspended in 100 μL binding buffer, then incubated with FITC-labelled antibody against Annexin V according to the manufacturer's protocol (BioLegend, 640922). Stained cells (1×10^4 per sample) were analyzed with Attune NXT flow cytometer.

Functional assessment in Ba/F3 and MCF10A cells

MCF10A cell line was obtained from the ATCC (CRL-10317) and Ba/F3 cell line was provided with M.D. Anderson Characterized Cell Line Core facility. The functional effects of *PIK3CA* mutations were assessed in Ba/F3 and MCF10A by survival assays as previously described(2). Cells were transfected with WT or *PIK3CA* mutants then cultured for 4 weeks and harvested for CellTiter-Glo viability assays. The relative cell viability for each mutant was calculated by the normalization to a range of 1 to 100, where WT *PIK3CA* is 1 and the positive control (a canonical mutant *PIK3CA* H1047R) is 100.

Functional assessment in HeLa cells

HeLa cell line was obtained from ATCC (CCL-2). Mutations were functionally characterized using an in vitro cell-based assay based on activation of signaling of mutants as previously described(3). *PIK3CA* mutations (MT) were generated in the wild-type (WT) expression vector then transfected into a live-cell assay with a fluorescently tagged FOXO1 that is a component of the PI3K/AKT pathway and which shuttles from the nucleus to the cytoplasm upon pathway activation. HeLa cells were then fixed and scanned by a fluorescent microscope to detect reporter localization that generated nuclear-to-cytoplasmic ratios (NCR) to provide comparisons of signaling activity for each mutant. NCR values were normalized and scored according to the activation levels of WT *PIK3CA* and the H1047R mutation, so that 0 represented WT activity and 1 was the activity of the *PIK3CA* H1047R. This was achieved using standard rescaling methods: score = (MT - *PIK3CA* WT)/(*PIK3CA* H1047R - *PIK3CA* WT), where MT is the reported NCR of the studied mutation condition and WT is the reported NCR of the wild-type condition.

Supplementary references

1. Lui VW, Peyser ND, Ng PK, Hritz J, Zeng Y, Lu Y, Li H, Wang L, Gilbert BR, General IJ, et al. Frequent mutation of receptor protein tyrosine phosphatases provides a mechanism for STAT3 hyperactivation in head and neck cancer. *Proc Natl Acad Sci U S A*. 2014;111(3):1114-9.
2. Dogruluk T, Tsang YH, Espitia M, Chen F, Chen T, Chong Z, Appadurai V, Dogruluk A, Eterovic AK, Bonnen PE, et al. Identification of Variant-Specific Functions of PIK3CA by Rapid Phenotyping of Rare Mutations. *Cancer Res*. 2015;75(24):5341-54.
3. Zimmerman L, Zelichov O, Aizenmann A, Barbash Z, Vidne M, and Tarcic G. A Novel System for Functional Determination of Variants of Uncertain Significance using Deep Convolutional Neural Networks. *Sci Rep.* 2020;10(1):4192.

Full unedited gel for Figure 2A

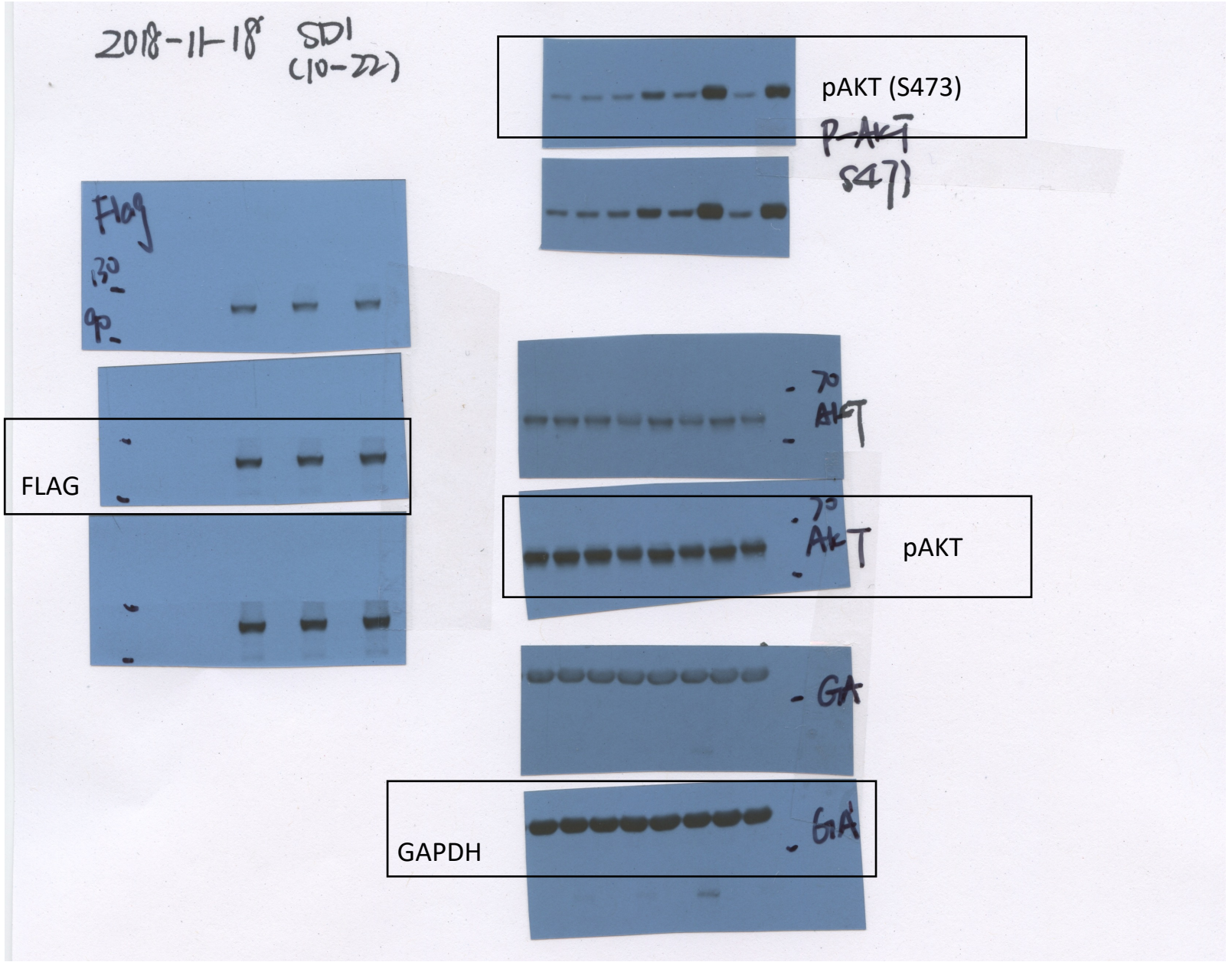

Full unedited gel for Figure 3B

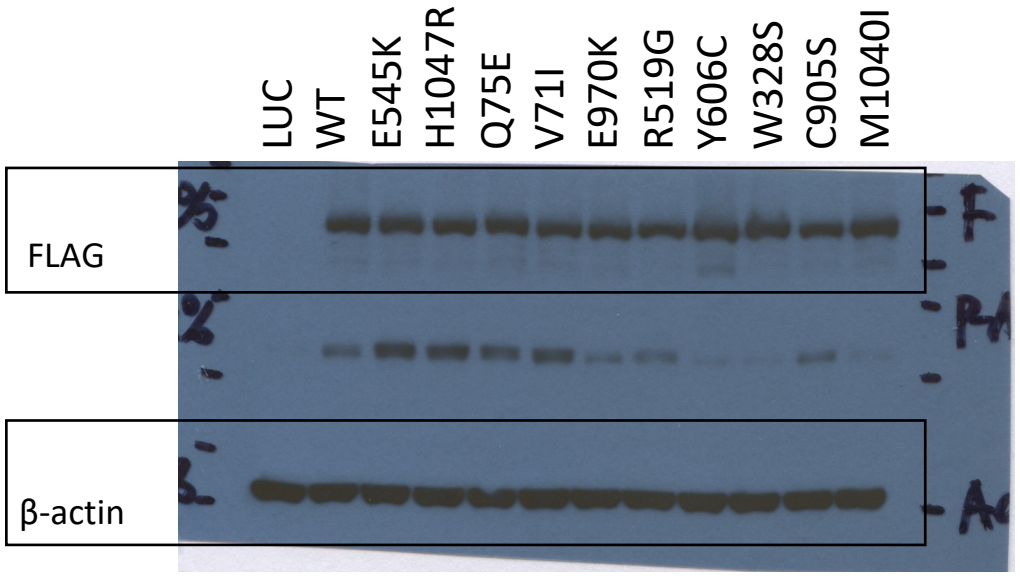

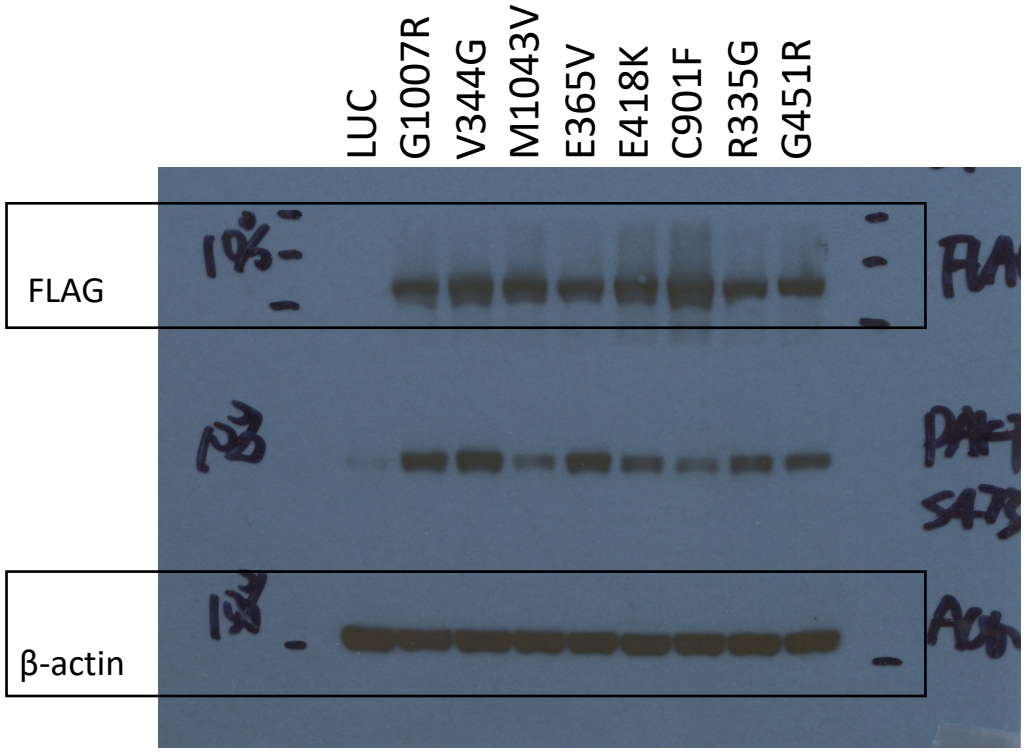

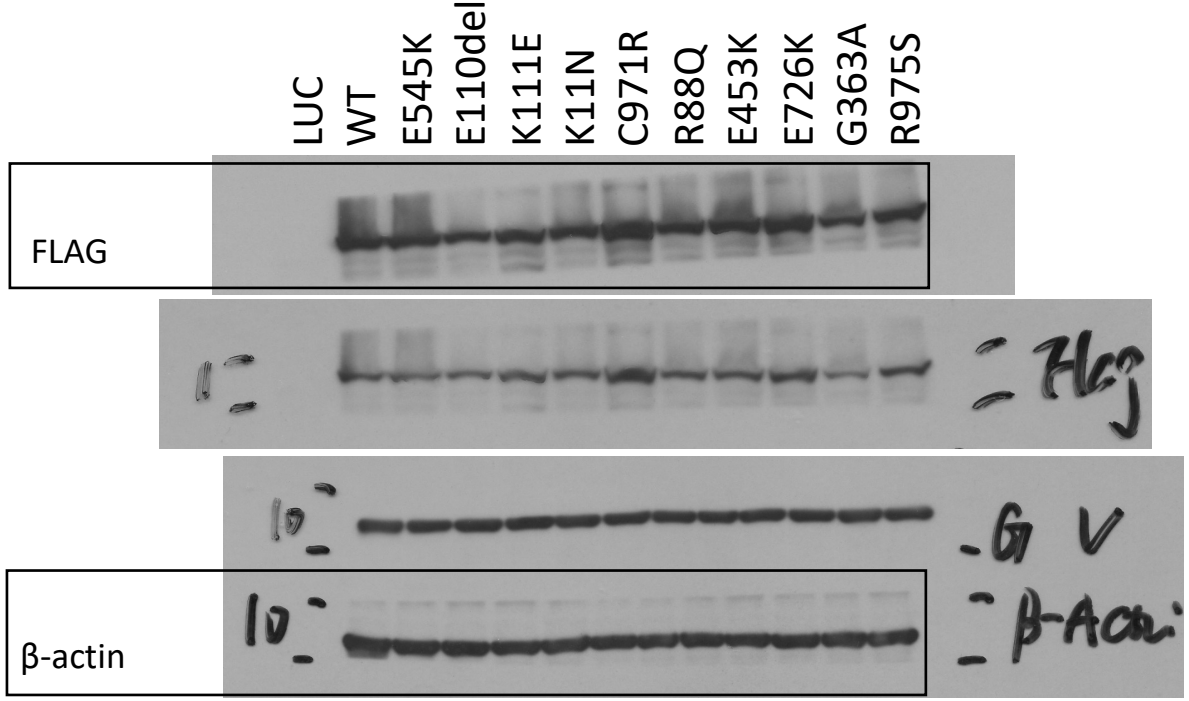

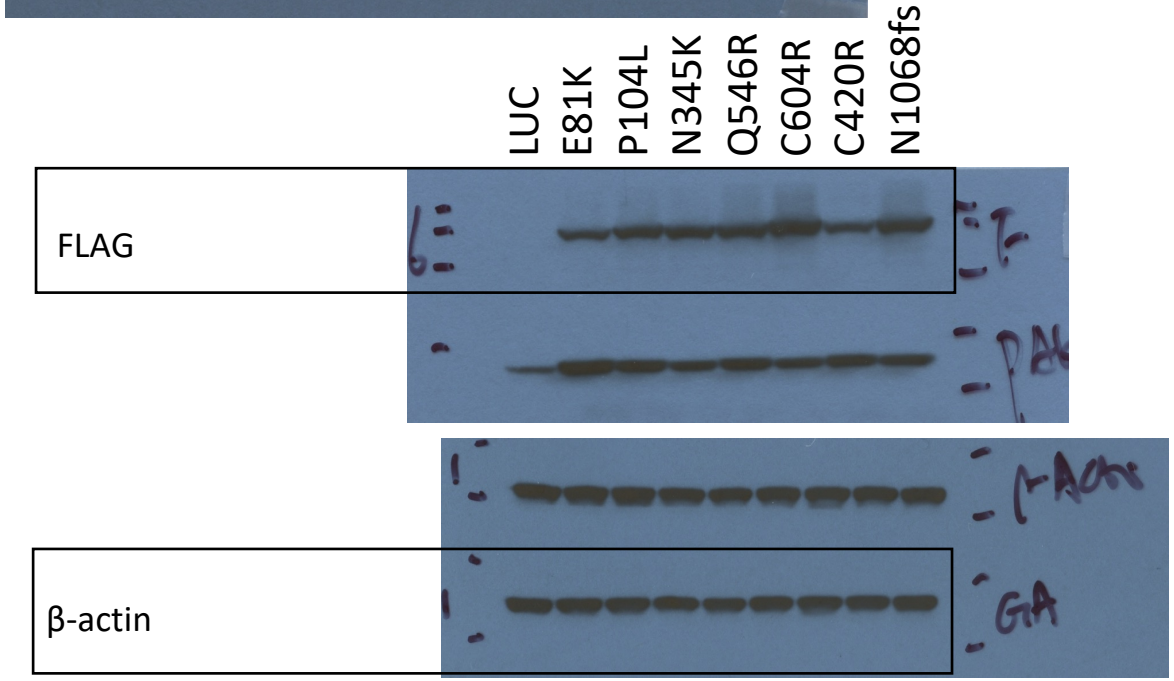

Full unedited gel for Figure 5B

Panel (left)

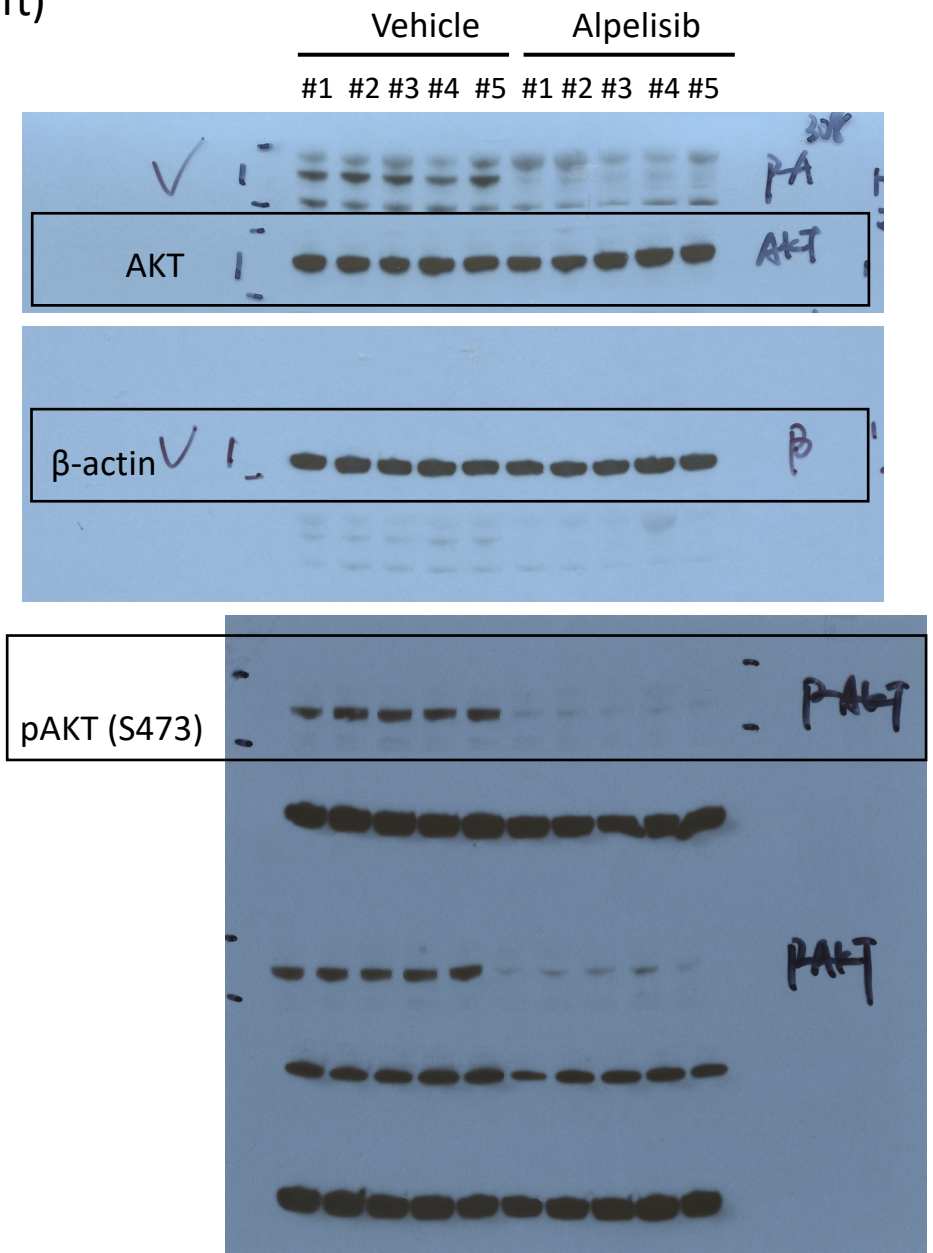

Panel (Right)

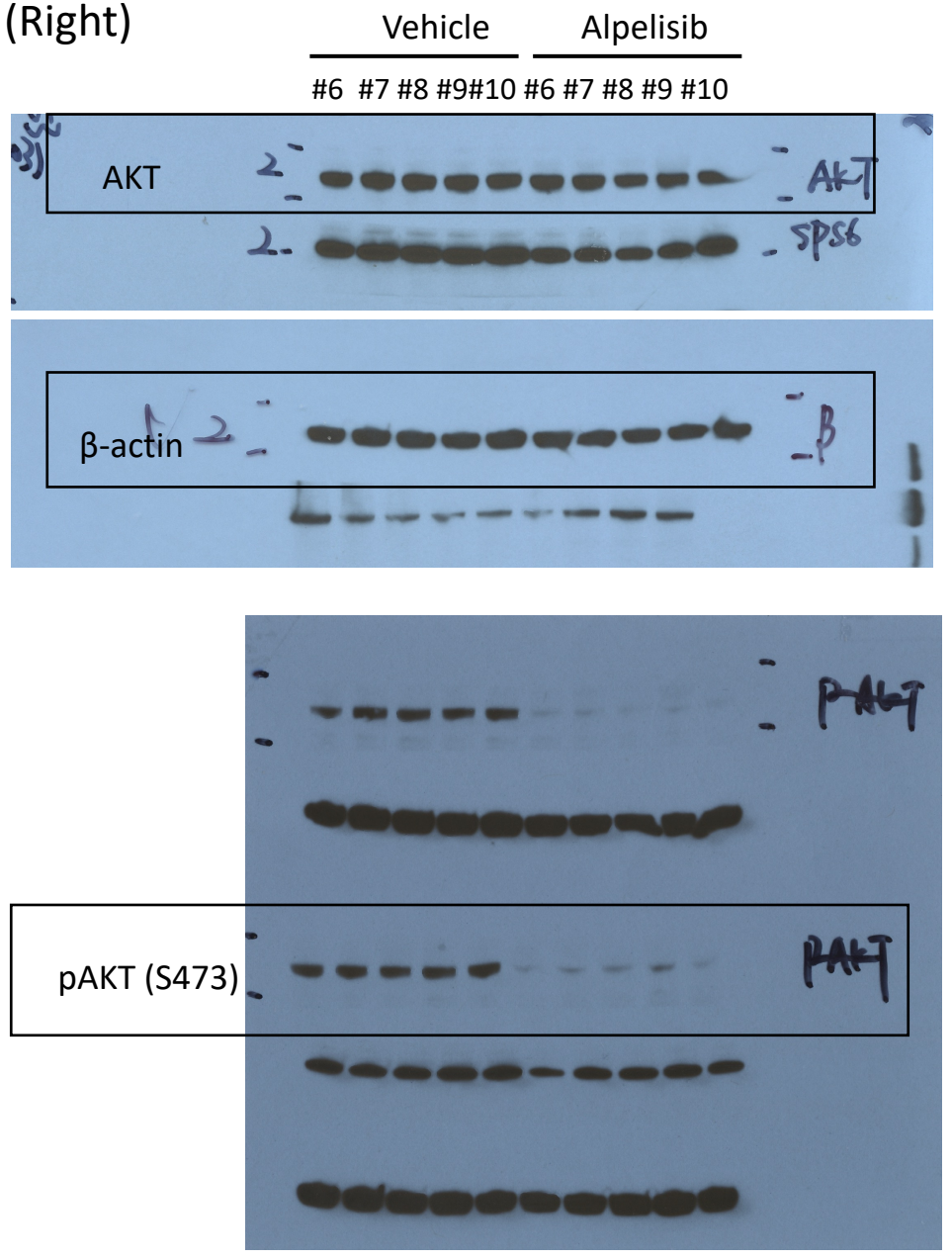

Full unedited gel for Figure 5D

Panel (left)

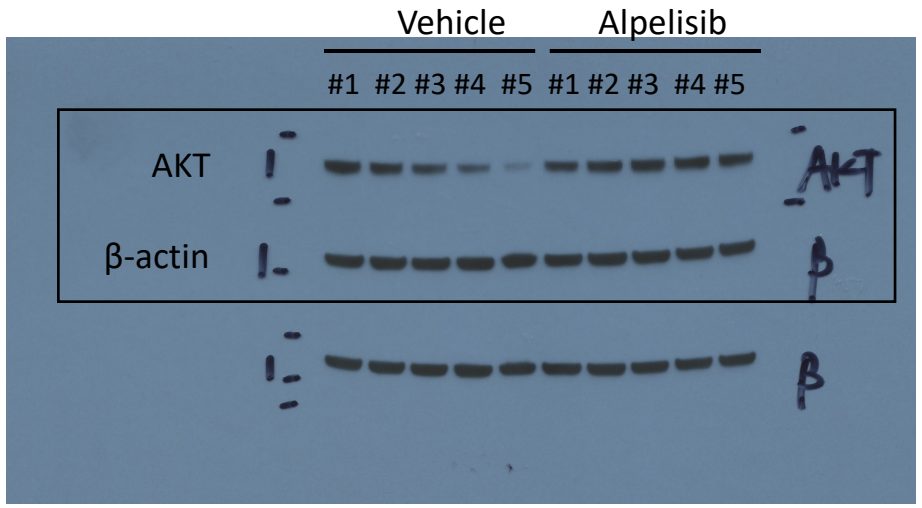

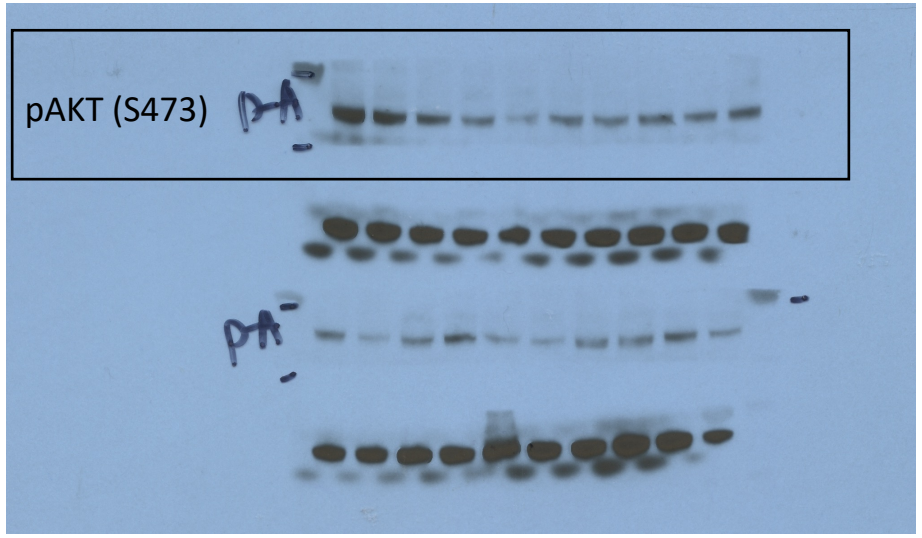

Panel (Right)

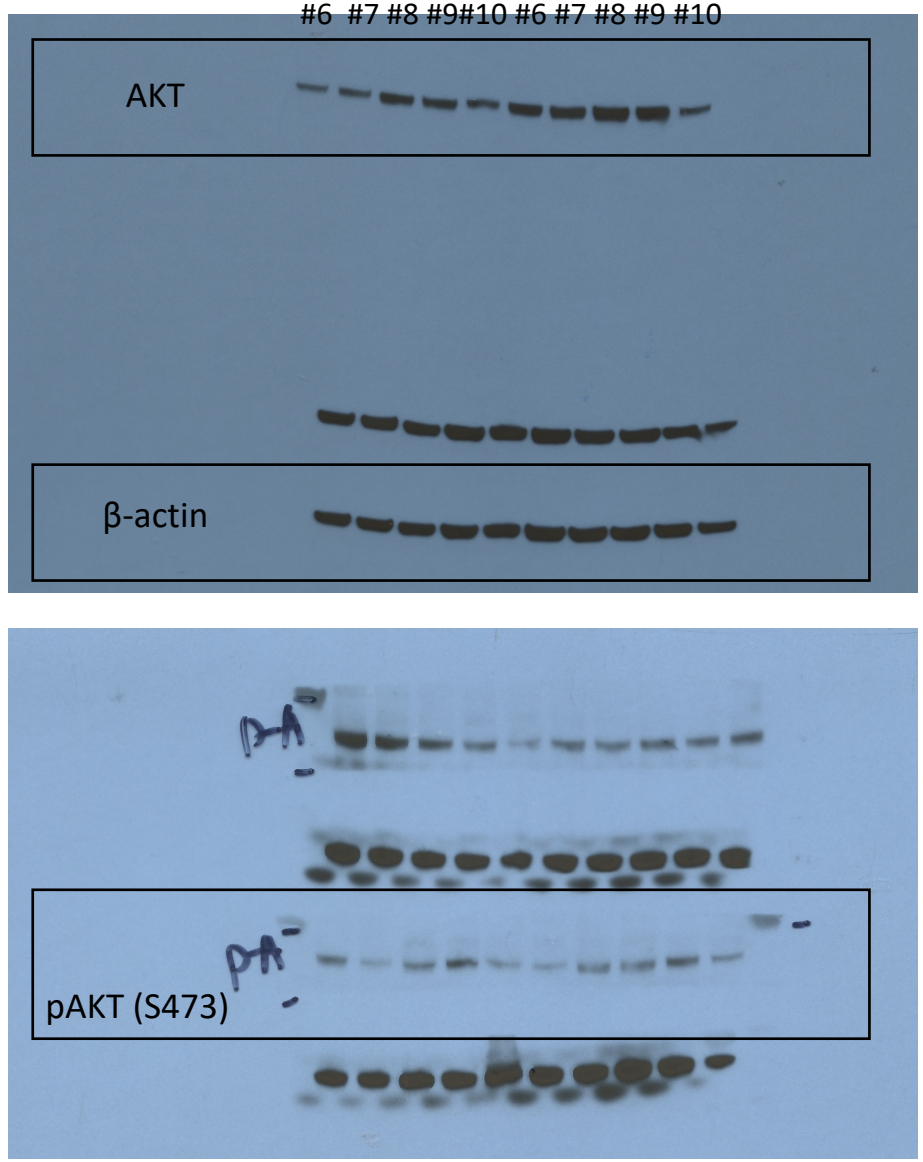

Full unedited gel for Supplemental Figure 4A

Panel (left)

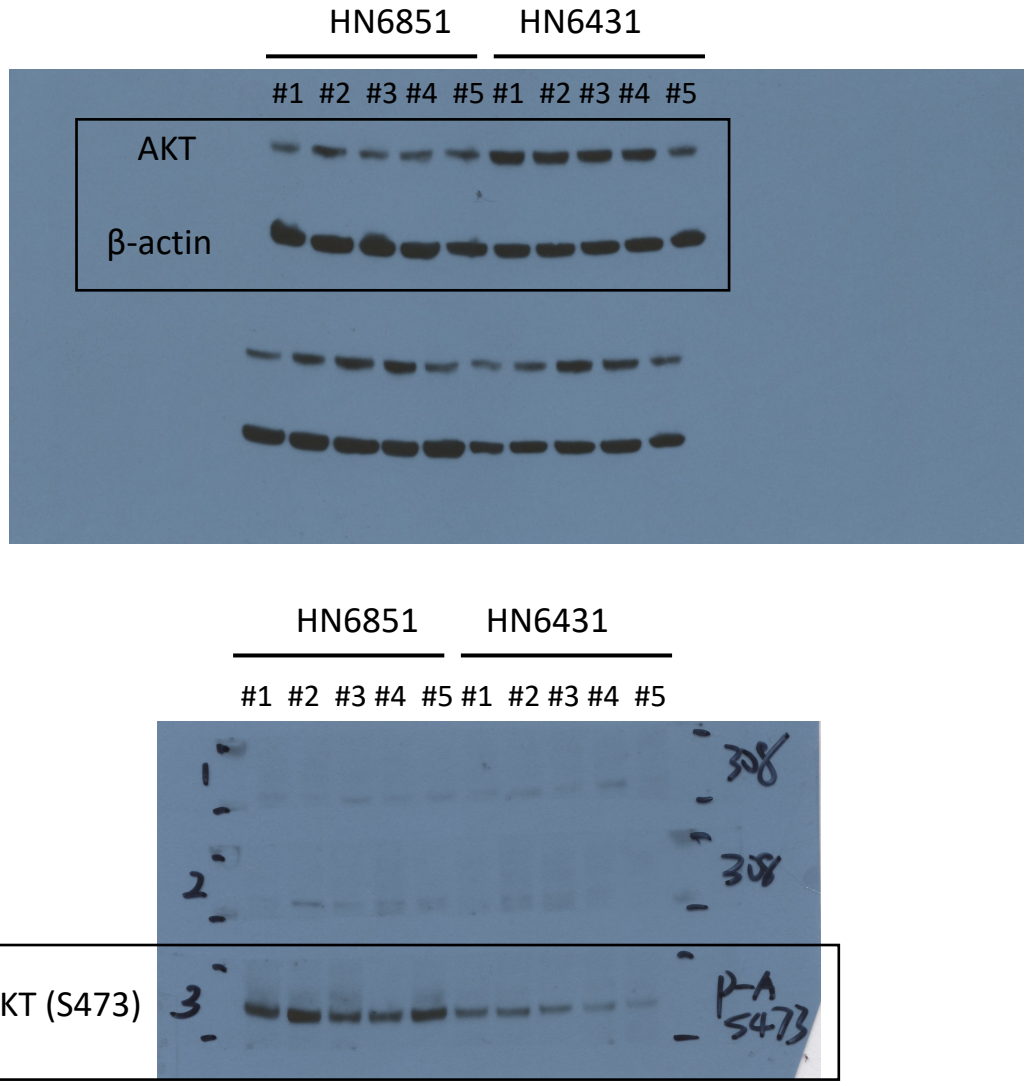

Panel (Right)

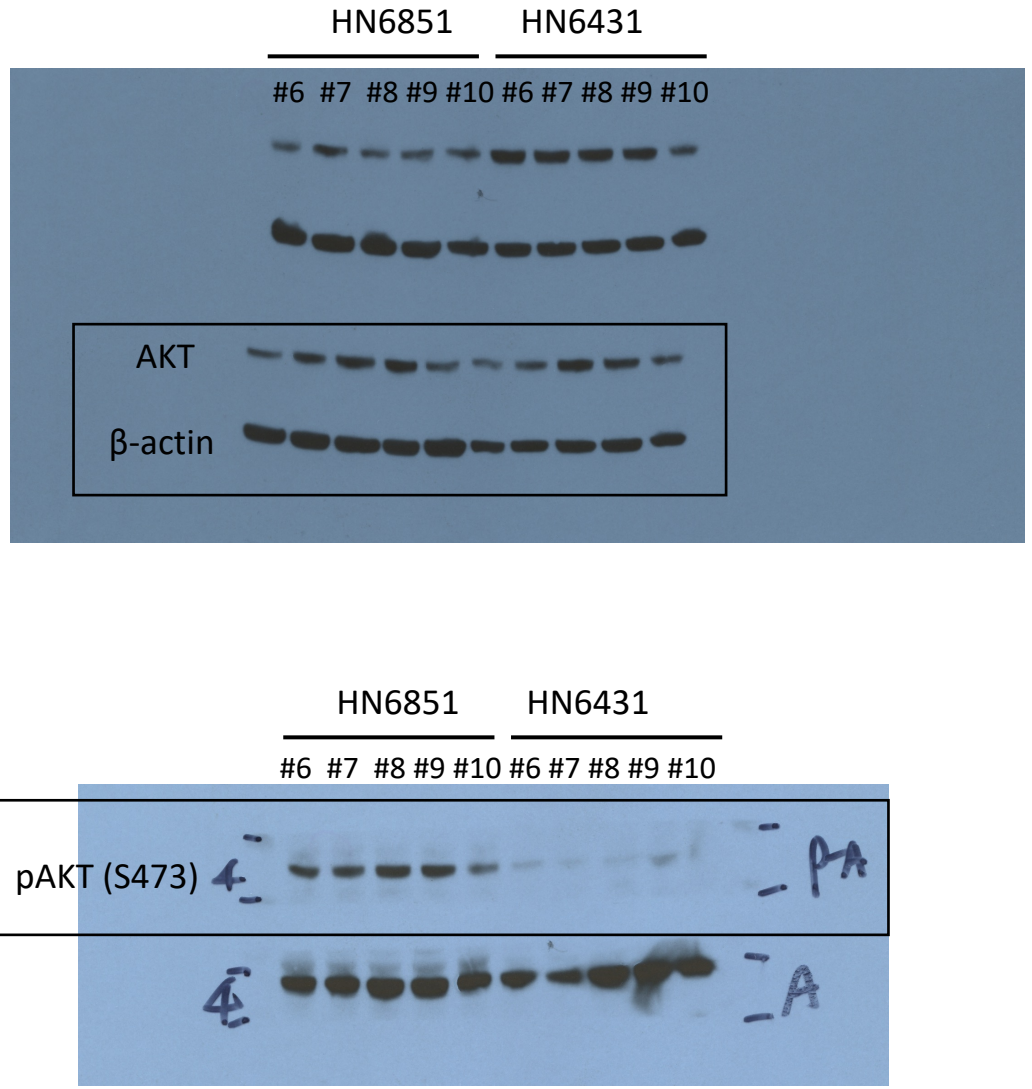

Full unedited gel for Supplemental Figure 4B